Int. J. Electrochem. Sci., 8 **(2013)** 12600 - 12612

International Journal of
ELECTROCHEMICAL
SCIENCE
www.electrochemsci.org

Inhibition of Carbon Steel CO_2 Corrosion in High Salinity Solutions

A.Y. Kina, J.A.C. Ponciano

Corrosion Laboratory, Materials and Metallurgical Engineering Program, COPPE, Rio de Janeiro Federal University, Ilha do Fundão, Technology Center, Rio de Janeiro – RJ, Brasil

Received: 20 August 2013 / *Accepted:* 4 October 2013 / *Published:* 20 October 2013

Corrosion inhibitors designed to prevent general carbon dioxide corrosion in carbon steel were investigated. The environment considered were two high salinity solutions, denominated as W_1 and W_2, which were kept at room temperature and had a pH of 4.8 and 5.6, respectively. The performance of 2-mercaptopyrimidine and 4,6-diamine-2-mercaptopyrimidine was assessed using electrochemical and weight loss tests. Mercaptopyrimidines were revealed to be mixed-type inhibitors that predominantly influenced the anodic process on the interface. The inhibition efficiency can be monitored by corrosion potential measurements. It was concluded that 2-mercaptopyrimidine presented better inhibition than 4,6-diamine-2-mercaptopyrimidine in the tested conditions.

Keywords: Corrosion inhibitor; Brine; CO_2 corrosion; Mercaptopyrimidine.

1. INTRODUCTION

Carbon dioxide corrosion is a relevant issue to the oil and gas sectors. This acid gas in aqueous environment is a corrosive specie that has caused several failures related to oil and gas pipeline [1] [2] and occur at all stages of production from downhole to surface equipment and processing facilities [3]. There are many variables associated with the CO_2 corrosion process, such as pH, temperature, pressure, flow, steel composition, inhibitor, brine chemical composition, surface films, etc [4]. Carbon dioxide corrosion has been studied by many researches and offer insights into the various complex processes occurring in CO_2 corrosion [5-7]. The first and most widely used model for predicting CO_2 corrosion of carbon steel in wells and pipelines was proposed by Waard and Millians [6], according to them the corrosion rate of carbon steel increases with an increase of the this acid gas partial pressure. Linter and Burstain [8] studied the action of CO_2 in the corrosion of low alloy and stainless steel, immersed in chloride and sulfate aqueous solution that had a pH 4. They conclude for those metals the electrochemical reduction of carbonic acid is unfavorable thermodynamically, when compared to other possible reactions like the hydrogen reduction and the water reduction. The presence of carbon dioxide in a brine solution can also promote formation of a layer on the metal surface. This scale is mainly formed by calcium carbonate ($CaCO_3$) and iron carbonate ($FeCO_3$). The formation of a layer on the metal surface will depend on the brine concentration, pH, temperature and other parameters. This layer can be protective or not, it would depend on the homogeneity, the porosity, the tenacity, the thickness, the adherence and the nature of the corrosion layer. [2][4-12].High-salinity CO_2 environments are of interest. Many research programs have addressed CO_2 corrosion. However, only a few references presenting data about CO_2 environments combined with high salinity can be cited. This specific condition is expected to occur in pre-salt oil and gas production areas on the Brazilian coast.

The salt content of a typical analysis of water wells is approximately 22% by weight, and this composition cannot be treated as an isolated case. Nesic reports that waters encountered in Texas oil wells with a salt content of 23 wt% are not uncommon. The author report that salt crystals can be observed inside the production tubing, meaning the salt concentration could be near saturation [13].

Most CO_2 corrosion inhibitor studies address low salt concentrations, within the range of 1 wt% to 3.5 wt% sodium chloride (NaCl) [13-16]. Under the conditions investigated here, the extremely high calcium content must be noted.

Organic compounds containing nitrogen, sulfur and oxygen atoms are widely used as corrosion inhibitors [17-20]. The performance of nitrogen-containing compounds, for example, pyrimidine derivatives, has been studied by many researchers in acid environments [20-23]. They usually adsorb on metallic surfaces, generating a protective film that interferes with electrochemical corrosion reactions [23].

Mercaptopyrimidine has emerged as a promising corrosion inhibitor, not only because it is a nonpoisonous material [23] but also because it seems to inhibit CO_2 corrosion when used in very low concentrations [20]. Although mercaptopyrimidine derivatives have been recently tested in CO_2 media, and showed efficiencies up to 99% [19] [23,25] in acid environments, there is no published study that addresses high-salinity solutions.

In this paper, results obtained with 2-mercaptopyrimidine (2-MP) and 4,6-diamine-mercaptopyrimidine (4,6-DMP), both tested as CO_2 corrosion inhibitors, will be presented. The methodology used is based on electrochemical and weight loss techniques.

2. EXPERIMENTAL

Two types of testing methodologies were used in this research. Weight loss experiments and electrochemical tests were carried out to measure the uniform corrosion rate of carbon steel samples. Polarization Curves and Electrochemical Impedance Spectroscopy (EIS) were used to assess the electrochemical response of the material under the same conditions. The results obtained with both methodologies were compared.

2.1. Material and corrosive solution

Table 1 describes the composition of the carbon steel used in the tests. This material was machined to fabricate the weight loss coupons and electrochemical working electrodes (WEs).

Table 1. Chemical composition of the Carbon steel.

Carbon Steel	C	Mn	P	S
% weight	0.075	0.52	0.025	0.017

The 2-MP (98%) and 4,6-DMP (99%) were tested as CO_2 corrosion inhibitors in concentrations equal to 5 mg/L, 10 mg/L and 25 mg/L.

Table 2 shows the composition of the first saline synthetic solution prepared using distilled water and analytical grade reagents (W_1 solution). The salt content of this brine was 22% by weight and simulates the formation water encountered in oil wells. To assess the influence of the calcium in the inhibitor efficiency due to the formation of a layer on the metal surface a second solution, denominated as W_2, was prepared. This second electrolyte was a modification of the W_1 solution, where the 40.00 g/L of calcium chloride was removed from the original composition and was replaced by 42.12 g/L of NaCl to keep the chloride concentration constant.

In two individual cells, with a working volume of 250 mL, the W_1 and W_2 electrolytes were saturated with CO_2, by bubbling the gas for 1 hour. After the saturation with carbon dioxide, the pH's of the brines were 4.8 and 5.6 at 298 K, respectively. To avoid oxygen entry and to ensure CO_2 saturation, pure acid gas was continuously bubbled in the solution during tests.

Table 2. Composition of the synthetic solution W_1.

Electrolyte	Concentration (g/l)
NaCl	224.90
$BaCl_2$	0.0391
KCl	7.5450
Na_2SO_4	0.5000
$NaHCO_3$	0.5310
$MgCl_2*6H_2O$	9.8850
$CaCl_2$	40.000
$SrCl_2*6H_2O$	4.5900

2.2. Polarization tests

The polarization measurements were obtained by employing a conventional three-electrode glass cell attached to a digital AUTOLAB 302N potentiostat. A saturated calomel electrode (SCE) was used as a reference. The counter electrode was a Pt wire placed close to the working electrode. The working electrode was machined from carbon steel.

The carbon steel electrode was prepared by embedding the carbon steel plate in epoxy resin and exposing a flat surface of approximately 1 cm^2 to the electrolyte. Prior to each measurement, the electrode surface was mechanically abraded by sandpaper up to #600 grit and then rinsed with ethanol and finally dried in hot air. Polarization curves were recorded using a constant sweep rate of 1 mV s^{-1}, within the limits defined as -300 to +300 mV versus corrosion potential (E_{corr}).

The measurements were started only after the WE had reached a steady corrosion potential after approximately 1h of immersion in the synthetic solution saturated with CO_2 at 298 K. Inhibitor performance using polarization curves (η_P %) were evaluated using the following equation (1):

$$\eta_P\% = \frac{(I_{corr(0)} - I_{corr(I)})}{I_{corr(0)}} \times 100 \qquad (1)$$

where $I_{corr(0)}$ is the corrosion current obtained without the addition of the inhibitor and $I_{corr(I)}$ is the corrosion current with different concentrations of each inhibitor tested.

2.3. Electrochemical Impedance Spectroscopy (EIS)

Using the same apparatus of the polarization test, the EIS measurements were performed at open corrosion potential, E_{corr}, within the frequency range 10^3 Hz – 2 mHz, with a signal amplitude perturbation of 10 mV. Potentiostatic control was used, and all measurements were carried out at the corrosion potential.

A Nyquist representation of impedance data was used, and the diagram was analyzed by using the FRA software. The polarization resistance (R_p) was then obtained from fitting the Nyquist plot using the software. R_p can be defined as a threshold value of the impedance corresponding to the lower frequency limit according to equation (2).

$$R_P = \lim_{\omega \to 0} Z \qquad (2)$$

where Z represents the impedance value and ω is the applied frequency.

2.4. Weight loss tests

Carbon steel coupons were machined to obtain rectangle surfaces with dimensions of 27.3 x 25.9 x 1.0 mm. These coupons were prepared before immersion by surface sandblasting, cleaned with ethanol, dried in hot air and, finally, weighed on a balance with 0.1 mg precision. The tests were performed according to ASTM practice standard G-31 [26].

Corrosion rates (C_R) were determined after 24 hours of immersion in the simulated water solutions. After the experiment, samples were chemically treated to remove all corrosion products. Clark solution, consisting of 1000 mL of hydrochloric acid, 20 g of antimony trioxide (Sb_2O_3) and 50 g of stannous chloride ($SnCl_2$), was prepared according to ASTM practice standard G-1 [27]. The specimens were immersed in this solution for 40 seconds, rinsed with water, cleaned with ethanol in an ultrasonic bath for 10 minutes, dried in hot air and, finally, weighed. Three identical specimens were processed in each experiment. The standard deviation of the measurements was approximately 0.001 mm/year. The mean value was reported and used for further data processing. The corrosion rate (mm/year) was calculated following the equation in ASTM practice standard G-31 [26]. An additional control sample was used to minimize errors in the weight loss calculation due to the cleaning procedures.

The efficiency $\eta\%$ was calculated by:

$$\eta\% = \frac{(C_{R0}-C_{Ri})}{C_{R0}} \times 100 \qquad (3)$$

where C_{R0} is the corrosion rate without an inhibitor and C_{Ri} is the corrosion rate with an inhibitor.

Carbon steel weight loss was evaluated by the NACE-RP0775 [28] standard. This document classifies general corrosion rate values lower than 0.120 mm/year as moderate corrosion. This value will be considered as an acceptance criterion for the inhibitors.

2.5. Surface analysis

The carbon steel specimens used for surface morphology examination were previously mechanically abraded by sandpaper up to #600 grit and rinsed with ethanol. Then they were immersed in W_1 solution saturated with CO_2 in the absence and presence of 10 mg/L of 2-MP and 4,6-DMP for 24 h. After the immersion time the specimens were rinsed with distilled water and in ethanol for 10 minutes in an ultrasonic bath to remove any corrosion products and avoid salt crystallization from the highly saline solution prior to imaging. All micrographs of the corroded carbon steel specimens were taken at a magnification of 2000x.

The analysis was performed on a Leo 940A (ZEISS) scanning electronic microscope operating in 20 kV in a secondary electron imaging mode.

3. RESULTS

3.1. Weight Loss Test

Table 3 shows the weight loss results obtained after 24 h of exposure in W_1 solution. It can be observed that the addition of mercaptopyrimidines to the solution reduced the corrosion rate compared with the blank condition (C_{R0}).The efficiency of the inhibitors increases with the increase of the inhibitor concentration up to 10 mg/L. Higher concentrations will lead to lower efficiencies. Similar behavior was observed by He et al. in a research studying thiourea as a CO_2 corrosion inhibitor in a saline environment [29]. It was evident that the compound 2-mercaptopyrimidine presented a higher inhibiting efficiency than the 4.6-diamine-mercaptopyrimidine. In the inhibitor concentration of 10 mg/L the carbon steel corrosion rates were respectively 0.1052 mm/year and 0.1582 mm/year.

However, it should be noted that only the 2-MP achieved the results considered to be moderate values for the uniform corrosion rate according to the NACE-RP0775 standard [28].

The corrosion rate in a blank solution without inhibitors is 0.3695 mm/year, which is considered to be severe corrosion according to the same NACE-RP0775 standard [28]. The corrosion rate in blank conditions could be higher, if the carbonate and corrosion products were not present in the solution. This reduction effect could be explained by the formation of a protective layer on the carbon steel surface. This layer can be protective or not, depending on many additional factors [2][8-11].

Table 3. Weight loss results of tested compounds in static conditions after 24 h of immersion at room temperature in W_1 solution saturated with CO_2.

Compound	Concentration (mg/l)	C_R (mm/year)	η%
Blank	0	0.3695	-
2-MP	5	0.1248	66.23
	10	0.1052	71.54
	25	0.1269	65.66
4.6-DMP	5	0.1892	48.78
	10	0.1582	57.18
	25	0.2403	34.96

To assess the influence of the calcium in the efficiency of mercaptopyrimidines as corrosion inhibitors, the carbon steel was immersed in W_1 and W_2 solution with the inhibitors concentrations of 5 mg/L, 10 mg/L and 25 mg/L. After 24 h of immersion, the same tendency toward an optimum concentration was observed (Figures 1(A) and (B)).

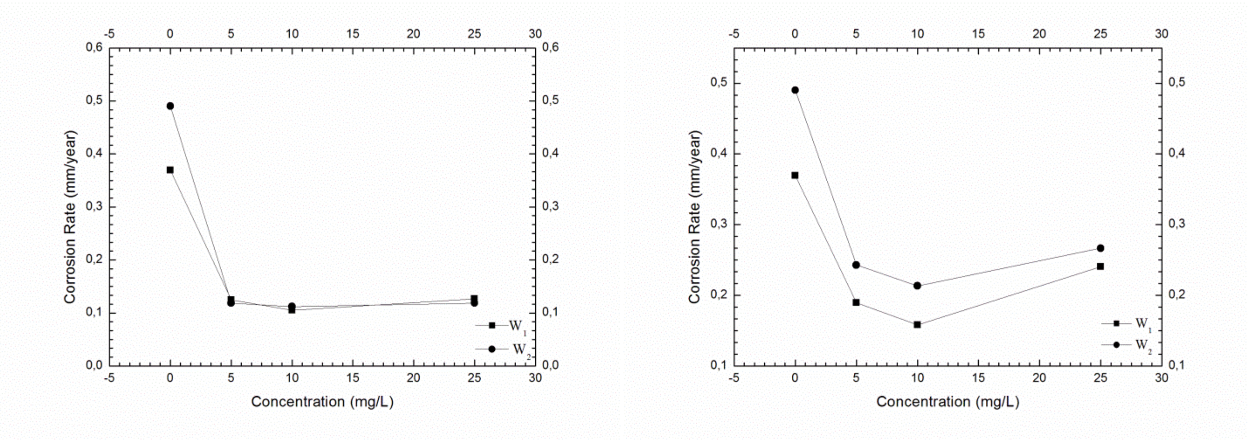

(A) (B)

Figure 1. Carbon steel corrosion rate after 24 h in presence of 5 mg/L, 10 mg/L and 25 mg/L of (A) 2-MP and (B) 4,6-DMP in W_1 and W_2 solutions saturated with CO_2 with at 25°C.

From the results, it can be concluded that W_2 solution can be considered a more aggressive environment than the W_1 solution, based on the corrosion rates obtained in blank solutions. The corrosion rate was 0.3695 mm/year for the W_1 solution and 0.4901 mm/year for the W_2 solution. This behavior may be related to the calcium carbonate layer on the steel surface formed in the W_1 environment that is not observed in W_2. The decrease in carbon steel corrosion rate influenced by the presence of calcium ion in the solution was also discussed by Jiag et. at. [30].

Solutions containing 2-MP appear to be less sensitive to the presence of $CaCl_2$ salt than 4,6-DMP. The corrosion rates observed in the solutions with 2-MP from experiments with and without this salt showed almost the same results. When using a concentration equal to 10 mg/L of this inhibitor, corrosion rates equal to 0.1052 mm/year for W_1 and 0.1120 mm/year for W_2 were achieved. In contrast, an analysis of weight loss tests comparing the results with 4,6-DMP in W_1 and W_2 solution showed an increase in the corrosion rate of 28.3% for concentrations of 5 mg/L, 34.9% for 10 mg/L and 10.9% for 25 mg/L (figure 1(B)).

3.2. Polarization Curves

Figure 2 and Figure 3 present the results of the polarization measurements in W_1 non-stirred conditions with different concentrations of the 2-MP and the 4.6-DMP, respectively.

It can be observed that the introduction of a corrosion inhibitor increased the corrosion potential to more positive values. The amplitude of this potential shift was dependent on the inhibitor concentration. This effect corresponding to a more positive corrosion potential was followed by a significant decrease of the anodic current. A similar effect can be observed from the analysis of the cathodic current.

Table 4. Electrochemical parameters from polarizations curves of carbon steel after 24 h of immersion in non-stirred W_1 solution in presence and absence of 2-MP and 4,6-DMP.

Inhibitor	Concentration (mg/l)	E_{corr} (mV_{SCE})	I_{corr} ($\mu A/cm^2$)	β_a (mV/dec)	β_c (mV/dec)	η_P %
Blank	0	-673	10.78	29.7	-204.4	-
2-MP	5	-632	1.55	38.3	-68.0	85.6
	10	-605	1.11	29.2	-84.4	89.7
	25	-664	1.89	42.7	-115.0	82.5
4,6-DMP	5	-635	2.79	39.7	-103.6	74.1
	10	-617	2.06	42.2	-194.8	80.9
	25	-642	4.32	37.0	-127.8	59.9

These results suggest that the compounds tested were mixed-type inhibitors, with the predominant influence on the anodic processes occurring at the electrochemical interface. The classification of these mercaptopyrimidine derivatives as mixed-type inhibitors was supported by other researchers that tested them as corrosion inhibitors [19] [24]. It is important to note that the inhibitive properties of the mercaptopyrimidines, expressed by the increase of the corrosion potential, were in agreement with the corrosion current (*I_{corr}*) values obtained from the polarization curves. The electrochemical parameters used to calculate the corrosion rates are shown in Table 4.

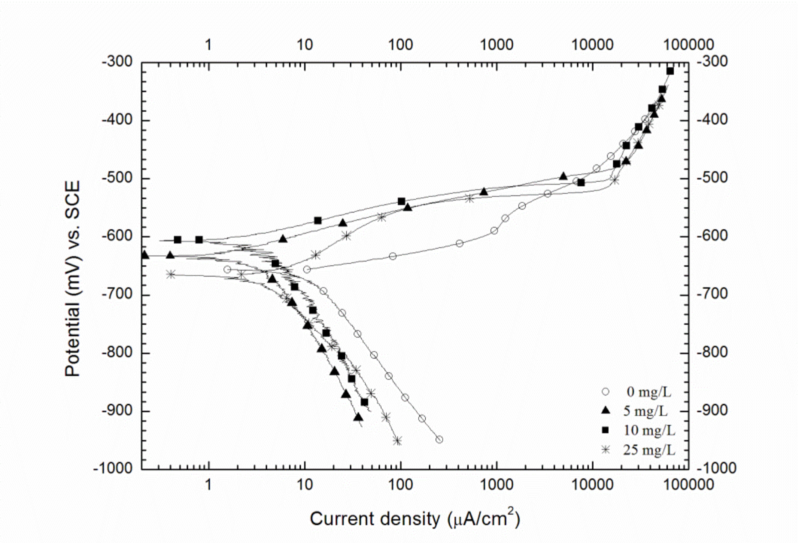

Figure 2. Polarization curves of carbon steel at room temperature with 0 mg/L (○), 5 mg/L (▲), 10 mg/L (■) and 25 mg/L (⁎) of 2-mercaptopyrimidine in W_1 solution saturated with CO_2 with at 25°C.

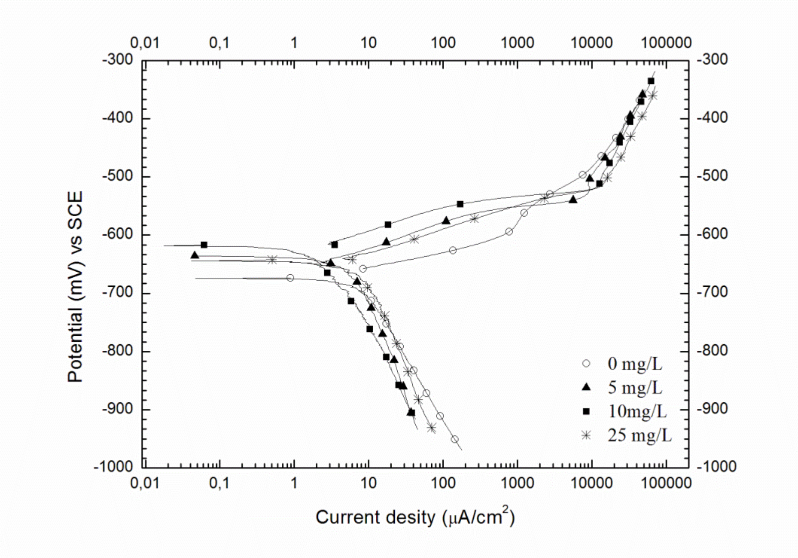

Figure 3. Polarization curves of carbon steel at room temperature with 0 mg/L (○), 5 mg/L (▲), 10 mg/L (■) and 25 mg/L (⁎) of 4.6-diamino-2-mercaptopyrimidine in W_1 solution saturated with CO_2 with at 25°C.

The optimum concentration of 10 mg/L corresponds to the best results extracted from the polarization tests for the inhibiting effect. These curves showed not only the lowest current density at room temperature (1.11 μA/cm^2 for 2-MP and 2.06 μA/cm^2 for 4,6-DMP) but also the highest corrosion potential (-605 mV_{SCE} for 2-MP and -617 mV_{SCE} for 4,6-DMP).

The results obtained from the polarization tests were qualitatively consistent with the weight loss tests [31]. The 2-MP at the concentration of 5 mg/L presented a corrosion current density of 1.55 μA/cm^2 and led to a corrosion rate of 0.1248 mm/year. When the concentration was increased to 10 mg/L, a reduction in the current density to 1.1 μA/cm^2 and a corrosion rate of 0.1052 mm/year were observed. This was the optimum concentration. Finally, for the concentration of 25 mg/L of 2-MP in Wo solution, the measured current density was 1.89 μA/cm^2, and the corrosion rate was 0.1269 mm/year.

The polarization curves showed better results for 2-MP than for 4,6-DMP, as observed in the weight loss experimental results (table 3 and table 4). Zucchi et. al.[32] and Khaled [33] report the same tendency of inhibitive performance for 2-MP and 4,6-DMP in acid solutions. The results informed by Zucchi were obtained by weight loss tests supported by quantum chemical approaches, and Khaled adopted a QSAR-based methodology. Both researchers compared the values of the highest occupied molecular orbital (HOMO) and the lowest unoccupied molecular orbital (LUMO), and they concluded that in most cases, the derivative that had the highest HOMO lowest-energy gap (LUMO - HOMO) and lowest dipole moment was expected to be the best corrosion inhibitor.

A comparison of the corrosion potential and the corrosion rate at the same concentration of tested inhibitors can be observed in figure 4 for 2-MP(A) and for 4,6-DMP (B). The higher was the corrosion rate, the lower was the E_{corr}. Again, the mixed-type inhibitor with the predominant influence of the anodic process on the surface was responsible for this behavior.

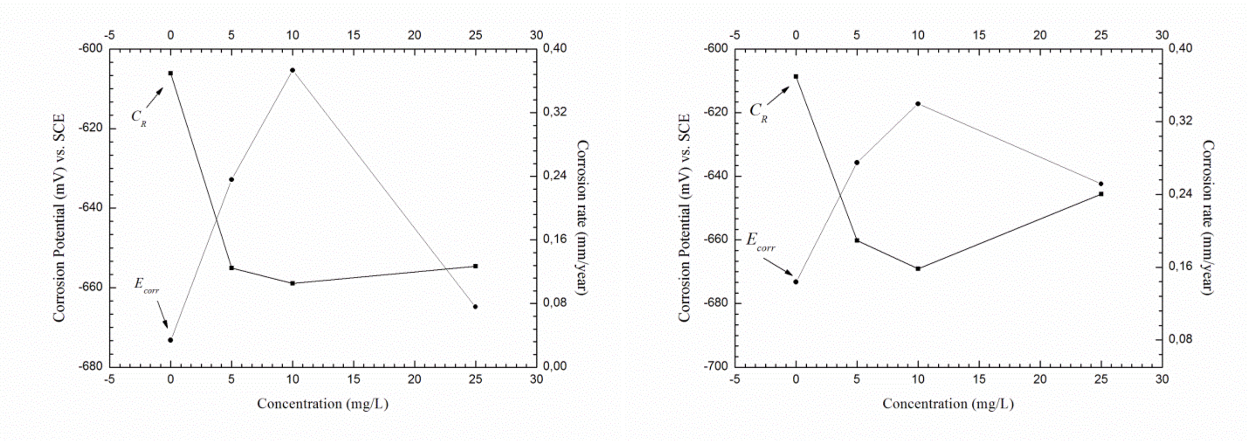

(A) (B)

Figure 4. Carbon steel corrosion rate and corrosion potential after 24 h in presence of 5 mg/L, 10 mg/L and 25 mg/L of (A) 2-MP and (B) 4,6-DMP in W_1 solution saturated with CO_2 with at 25^{o}C.

3.3. Electrochemical Impedance Spectroscopy (EIS)

Figure 5 shows the Nyquist plot of the EIS measurement of carbon steel immersed in W_1 solution for 1 h in absence and presence of 10 mg/L of 2-MP and 4,6-DMP. The impedance diagram obtained for W_1 in blank condition showed two a capacitive loop in the high-frequency range followed by a small inductive loop in the low-frequency range. The capacitive semicircle obtained in the higher-frequency range could be associated with double-layer capacitance and charge-transfer resistance, while the inductive semicircle at low-frequency is usually related to an adsorbed intermediate species formed during the dissolution of the electrode [34]. This behavior was also observed by others performing EIS studies in CO_2 media [34-37]. The inductive loop was attributed to active dissolution of the carbon steel, through intermediate species $FeOH_{ads}$, according to equation 5 of the mechanism:

$$Fe + H_2O \rightarrow FeOH_{ads} + H^+ + e^- \qquad (4)$$

$$FeOH_{ads} \rightarrow FeOH^+_{sol} + e^- \qquad (5)$$

$$FeOH^+_{sol} + H^+ \rightarrow Fe^{2+}_{sol} + H_2O \qquad (6)$$

In the presence of 10 mg/L of the inhibitors, only a capacitive loop was observed over all frequency ranges recorded. This loop showed an increase in the polarization resistance (R_p) suggesting an increase in inhibitor adsorption and reduction of the corrosion process.

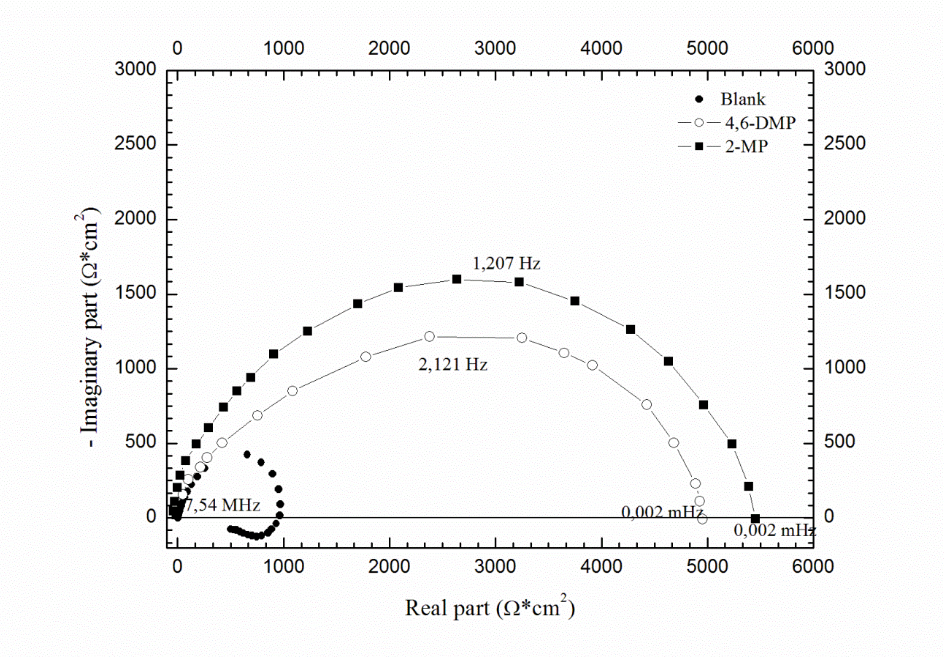

Figure 5. Nyquist plot of the EIS measurement of carbon steel immersed in W_1 solution for 1 h in (●) absence and presence of 10 mg/L of (■) 2-MP and (○) 4,6-DMP.

Table 5 describes the polarization resistance (R_p) values obtained from other inhibitors concentrations measurements. The highest values of R_p were observed in the concentration of 10 mg/L for 2-MP and 4,6-DMP, respectively. Additionally, the highest values of the corrosion potential (-605 mV_{SCE} for 2-MP and -617 mV_{SCE} for 4,6-DMP) were obtained at the same concentration of 10 mg/L for both inhibitors.

Table 5. Impedance measurement Results after 1 h of immersion in non-stirred W_1 solution in presence and absence of 2-MP and 4,6-DMP.

Compound	Concentration (mg/l)	R_p (ohm*cm^2)
Blank	0	432.95
2-MP	5	1787.27
	10	5427.09
	25	3167.15
4,6-DMP	5	2740.12
	10	4949.56
	25	2033.54

3.4. Surface analysis (SEM)

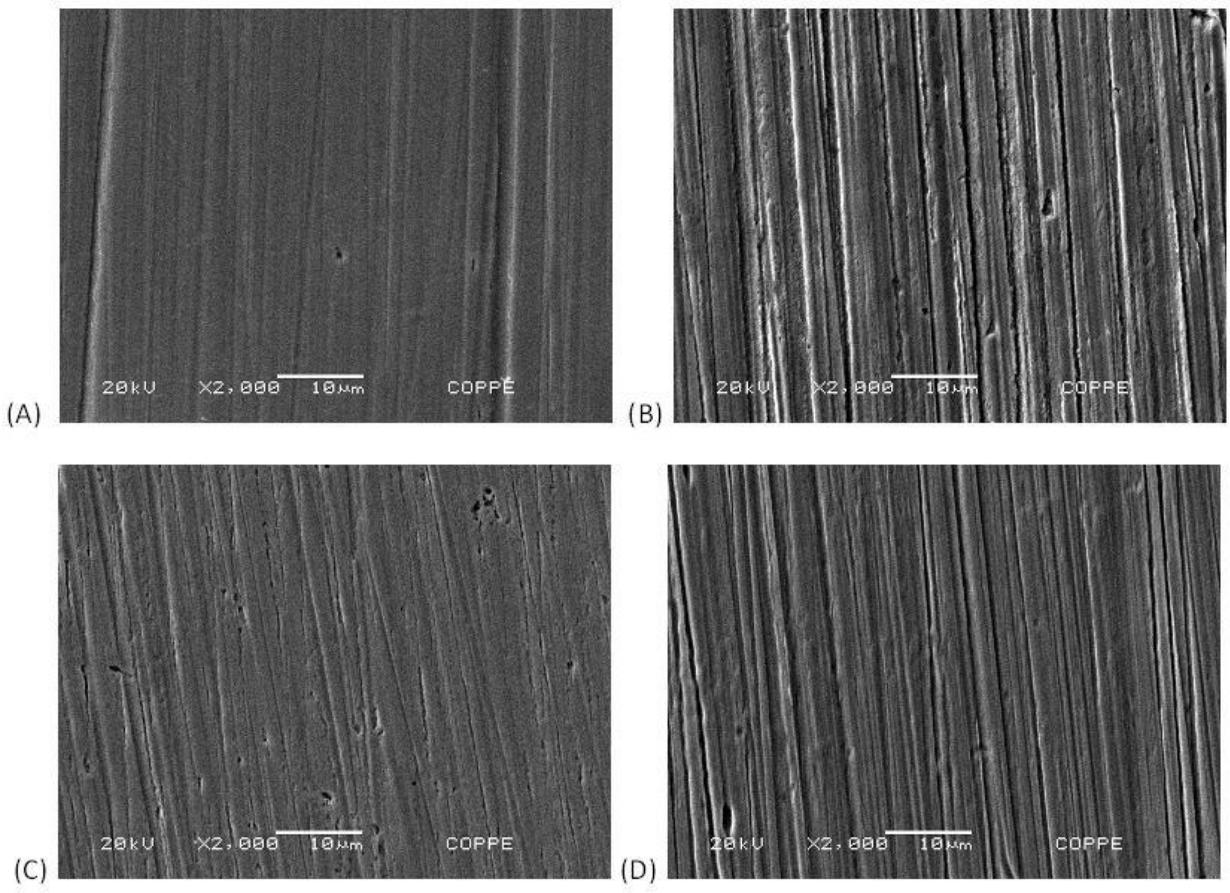

Figure 6. SEM micrograph recorded for carbon steel samples mechanically abraded by sandpaper up to #600 grit (A) and exposed for 24 h in W_1 solution saturated with CO_2 without (B) and with 10 mg/L of 2-MP (C) and 10 mg/L of 4,6-DMP (D) at 298 K.

Figure 6 shows an SEM micrograph recorded for carbon steel samples mechanically abraded by sandpaper up to #600 grit (A) and exposed for 24 h in brine without (B) and with 10 mg/L of 2-MP (C) and 10 mg/L of 4,6-DMP (D) at 298 K. The morphology in fig. 6 (B) shows a uniform corrosion of carbon steel in brine without inhibitor, initiating preferably through the existing grooves on the AISI A 36 surface that was mechanically abraded. The same tendency was noticed in brine with added inhibitors (fig. 5 (C) and (D)), with lighter intensity. The specimen surface immersed in brine with 2-MP was less corroded. These results corroborate the electrochemical analyses and weight loss measurements, where the inhibition efficiency of 2-mercapitopyrimidine produced the highest result.

4. CONCLUSION

1. The mercaptopyrimidines studied showed good inhibitive performances for the tested concentration range (5 mg/L – 25 mg/L) for CO_2 corrosion in high-salinity media, with an optimum efficiency of 71.54% for 10 mg/L in weight loss tests.
2. $CaCl_2$ salt does not seem to influence the remaining optimum concentration for either inhibitor, although the media becomes more severe in terms of the corrosion aspects (0.3695 mm/year for Wo and 0.4901 mm/year for Wo mod).
3. Results suggest that the compounds tested were mixed-type inhibitors, with the predominant influence on the anodic processes occurring at the electrochemical interface.
4. For both compounds the increase of inhibiting efficiency was accompanied by an increase in the open circuit potential.
5. The inhibitor 2-MP achieved better results in weight loss and electrochemical tests compared with the inhibitor 4,6-DMP. At a concentration of 10 mg/L, 2-MP presented a corrosion rate of 0.1052 mm/year, which is considered a moderate corrosion rate. These results were corroborated by the surface analysis that showed a less corroded sample surface that was immersed in brine with 2-MP.

References

1. M.B. Kermani, *Corros.*, 59 (2003) 659.
2. S. Nešić, *Corros. Sci.*, 49 (2007) 4308.
3. S.L. Fu, J.G. Garcia, A.M. Griffin, Nace Corrosion/96 Conference, paper 21, Corrosion/96, Denver, 1996.
4. J.L. Mora-Mendoza, S. Turgoose, *Corros. Sci.*, 44 (2002) 1223.
5. A. Ikeda, M. Ueda, S. Mukai, Nace Corrosion/83 Conference, paper 45, Corrosion/83, Houston, 1983.
6. C. De Waard, D.E. Milliams, *Corros.*, 31 (1975) 177.
7. M. Gao, X. Pang, K. Gao, *Corros. Sci.*, 53 (2011) 557.
8. B.R. Linter, G.T. Burstein, *Corros. Sci.*, 41 (1999) 117.
9. T. Li, Y. Yang, K. Gao, M. Lu, *J. Univer. Sci. and Technology Beijing*, 15 (2008) 702.
10. J.L. Crolet, N. Thevenot, S. Nesic, Nace Corrosion/96 Conference, paper 3, Corrosion/96, Denver, 1996.
11. F. Farelas, M. Galicia, B. Brown, S. Nešić, H. Castaneda, *Corros. Sci.*, 52 (2010) 509.

12. K. Gao, F. Yu, X. Pang, G. Zhang, L. Qiao, W. Chu, M., *Corros. Sci*., 50 (2008) 2796.
13. H. Fang, S. Nešić, B. Brown, S. Wang, Nace Corrosion/06 conference, paper 372, Corrosion/06, Houston, 2006.
14. F.G. Liu, M. Du, J. Zhang, M. Qiu, *Corros. Sci*., 51(2009) 102.
15. P.C. Okafor, X. Liu, Y.G. Zheng, *Corros. Sci*., 51 (2009) 761.
16. B. Wang, M. Du, J. Zhang, C.J. Gao, *Corros. Sci.*, 53 (2011) 353.
17. X. Jiang, Y.G. Zheng, W. Ke, *Corros. Sci*., 47 (2005) 2636.
18. F. Bentiss, M. Traisnel, J.C. Hornez, *Corros. Sci*., 41 (1999) 789.
19. W. Villamizar, M. Casales, J.G. Gonzales-Rodriguez, L. Martinez, *Mater. and corros*., 57 (2006) 696.
20. V.S. Reznik, V.D. Akamsin, Yu.P. Khodyrev, R.M. Galiakberov, Yu.Ya. Efremov, *Corros. Sci*., 50 (2008) 392.
21. G. Berecket, C. Öğretir, M. Yaman, E. Hür, *J. Molec. Struct*., 625 (2003) 31.
22. G. Gece, *Corros. Sci*., 50 (2008) 2981.
23. L. Wang, *Corros. Sci*., 43 (2001) 1637.
24. S.A. Abd El-Maksoud, A.S. Fouda, *Mater. Chem. and Phy*., 93 (2005) 84.
25. D.A. López, S.N. Simison, S.R. de Sánchez, *Corros. Sci*., 47 (2005) 735.
26. ASTM practice standard G-31 "Standard practice for laboratory immersion corrosion testing of metals", ASTM International, 2004.
27. ASTM practice standard G-1 "Standard practice for preparing, cleaning and evaluating corrosion test specimens", ASTM International, 2003.
28. NACE-RP0775 "Preparation,installation analysis, and interpretation of corrosion cupons in oilfield operations", NACE, Houston, 2005.
29. X.Y. He, H.Y. Deng, R. Li, X.D. Fei, H.Y. Wang, Z.Y. Deng, *Acta Metallur. Sinica*, 21 (2008) 65.
30. X. Jiang, Y.G. Zheng, D.R. Qu, W. Ke, *Corros. Sci.*, 48 (2006) 3091.
31. A.M. Alsabagh, M.A. Migahed, *Corros. Sci*., 48 (2006) 813.
32. I. Lukovits, E. Kálmán, F. Zucchi, *Corrosion*, 57 (2001) 3.
33. K.F. Khaled, *Corros. Sci*., 53 (2011) 3457.
34. G.A. Zhang, Y.F. Cheng, *Corros. Sci*., 51 (2009) 87.
35. J.B. Sun , G.A. Zhang , W. Liu , M.X. Lu, *Corros. Sci*., 57 (2012) 131.
36. C. N. Cao, *Corros. Sci*., 38 (1996) 2073.
37. A. B. da Silva, J. A. C. P. Gomes, E. D'Elia, M. J. C. Rezende, A. C. Pinto, B. N. M. Silva, B. V. Silva, *Int. J. Electrochem. Sci*., 8 (2013) 9317.